

The End-to-End Approach to Marine Ecosystem Modelling

by

Mandy Bunke

**Thesis submitted in fulfilment of the requirements for the
degree of MSc by Research**

**University of York
Department of Biology
March 2010**

Abstract

Traditionally compartments of the marine ecosystem have been modelled separately with focus depending on research issues and questions. The problem with these traditional approaches is that they might fail to capture events at an ecosystem scale and cannot replicate the internal ecosystem structure. The fragmentation might also fail to capture the effects of anthropogenic and environmental forcing. End-to-end modelling aims to represent the marine ecosystem as a whole to assess the combined effects that anthropogenic and environmental factors have on it.

This study used a simple non-spatial mathematical model with four state variables representing nutrients, phytoplankton, zooplankton and fish, to investigate the dynamic behaviour of the model. The three approaches of mathematical, graphical and numerical analysis were employed in the process of the study.

All three methods of analysis indicated the presence of two internal equilibrium points, of which one was observed to be stable. The interesting finding was that fish density is higher at the stable equilibrium point and that a basin boundary prevents the reaching of this equilibrium once fish density falls below a certain value. It was also observed that the mortality rate of fish was the main parameter influencing the behaviour of the system.

These findings are consistent with findings from other studies, and observations in exploited fisheries, which have described that processes such as fishing can make the ecosystem less stable. It can also give a possible reason for why some over exploited fish stocks have not recovered even after their exploitation was stopped.

Contents

	Page
Abstract	3
List of Figures	5
List of Tables	6
1. Introduction	7
1.1. Use of models in environmental management	7
1.2. Traditional types of models	7
1.3. Ecosystem models	8
1.4. End-to-end models	9
1.5. Mathematical models	12
1.6. Objectives	12
2. Methods	13
2.1. The models	13
2.1.1. The NP model	14
2.1.2. The NPZ model	15
2.1.3. The NPZF model	16
2.2. Mathematical analysis of model dynamics	17
2.3. Phase space analysis	18
2.4. Numerical integrations	18
3. Results	19
3.1. Mathematical analysis of model dynamics	19
3.1.1. The NP model	19
3.1.2. The NPZ model	20
3.1.3. The NPZF model	23
3.2. Phase space analysis	26
3.2.1. The NP model	26
3.2.2. The NPZ model	27
3.2.3. The NPZF model	30
3.3. Numerical integrations	33
3.3.1. The NP model	33
3.3.2. The NPZ model	34
3.3.3. The NPZF model	37
4. Discussion	44
4.1. The NP model	44
4.2. The NPZ model	44
4.3. The NPZF model	46
5. Conclusion	48
Acknowledgements	49
References	50

List of Figures

	Page	
Figure 1	Schematic of final model	13
Figure 2	NP phase space	27
Figure 3	NPZ phase space	28
Figure 4	NPZ phase space magnification	28
Figure 5	Shift of internal isocline	30
Figure 6	NPZF phase space	31
Figure 7	NPZF shift of internal isocline	33
Figure 8	NP numerical integration	34
Figure 9	NPZ numerical integration	35
Figure 10	NPZ phase space integrations	36
Figure 11	NPZF integrations starting higher than unstable equilibrium	37
Figure 12	NPZF phase space integrations	38
Figure 13	NPZF numerical integrations from starting values	39
Figure 14	NPZF phase space integrations from starting values	40
Figure 15	NPZF integrations from unstable equilibrium	41
Figure 16	NPZF phase space integrations from unstable equilibrium	41
Figure 17	NPZF integrations starting much higher than the stable equilibrium	42
Figure 18	NPZF phase space integrations	43

List of Tables

		Page
Table 1	Parameter values used in models	17
Table 2	Equilibrium points and eigenvalues in the NP model	19
Table 3	Equilibrium points and eigenvalues in the NPZ model	21
Table 4	Equilibrium points and eigenvalues in the NPZF model	24

I hereby declare that this thesis has been composed by myself and has not been accepted in any previous application for a degree. Information drawn from other sources and assistance received have been duly acknowledged.

Mandy Bunke

March, 2010

1. Introduction

1.1 Use of models in environmental management

Models have a history of being used in a variety of areas in environmental management. They are deployed in making decisions on water quality management (Benndorf and Recknagel, 1982; Vieira and Lijklema, 1989), population management for the conservation of species (Jongejans *et al.*, 2008; Shea *et al.*, 1998) and in assessing the impact of habitat fragmentation (Gehring and Swihart, 2003; Rantalainen *et al.*, 2008). Models are also readily employed to assess the impact of human actions on the environment. An example for this is the use of models to assess the impact of aquaculture on the marine environment (e.g. Stigebrandt *et al.*, 2004; Díaz López *et al.*, 2008). Models have proved to be a useful tool in environmental management because they make it relatively easy to test different management scenarios and to quantify their impacts (Travers, 2009).

1.2. Traditional types of models

In the marine environment, traditionally there have been two main branches of modelling, biogeochemical and fish production models (Cury *et al.*, 2008). These branches focus on components of the ecosystem, modelling them independently from the rest of the system, depending on research issues and questions (Franks, 2002; Latour *et al.*, 2003). Other components of the ecosystem, and the effects of abiotic factors, have largely remained unconsidered in the past (Travers *et al.*, 2007).

Biogeochemical models are developed to assess the dynamic forcing of the oceans and its impacts on the primary production and nutrient fluxes which occur (e.g. Franks, 2002). A common example for the modelling of fluxes in the marine ecosystem is the modelling of nitrogen, the main limiting factor in primary production, fluxes between the nutrient, phytoplankton and zooplankton compartments (e.g. Franks, 2002). Biogeochemical models, which are coupled to hydrodynamic models, can be used to assess environmental effects on plankton (e.g. Koné *et al.*, 2005). Biogeochemical

models only represent small compartments of the marine ecosystem so they cannot be used to assess the effects of fishing on the marine environment (Travers *et al.*, 2007).

Fish production models were originally studied because of the economic importance of the fish (Travers *et al.*, 2007). They focus on assessing the impact of fishing on exploited stocks. Initially the models focused on a single species (e.g. Andersen and Ursin, 1977). Later multi-species models were employed (first proposed by Pope, 1979) to advise in the management of fisheries. These models are based on equations for survival and catch and represent a cohort analysis of the exploited species. They may take predator interactions into account and explicitly model predation (Travers *et al.*, 2007). However, the single species approach has not been abandoned.

1.3. Ecosystem models

The problem with these traditional approaches is that they might fail to capture events at an ecosystem scale, and cannot replicate the internal ecosystem structure of the ecosystem (Cury *et al.*, 2008), due to their specific focus. This can be the case because a perturbation at any point in the ecosystem can propagate both up and down through the food web and too specific a focus may fail to identify cascading effects, which result from anthropogenic and environmental forcing (IMBER, 2005).

It has been long recognised that in addition to fishing, the abiotic environment has an influence on the dynamics of marine organisms. This was first mentioned by Hjort (1914) at the beginning of the last century. It is important to keep in mind that both the abiotic and anthropogenic factors are impacting the organisms at the same time and this should be taken into consideration when modelling is undertaken (Fennel, 2008; Travers *et al.*, 2007). It is important to take this into consideration because, as Harley *et al.* (2006) emphasized, the effects of a factor (e.g. climate) may amplify or reduce the effects of another factor (e.g. fishing). But a combination of both can also result in extreme changes that were never effected by the forcing of a single factor. It is thought that this combination of factors is probably at the origin of regime shifts that have been

observed in the past (Folke *et al.*, 2004). The direct effects of climate and fishing have been modelled for a long time. However, few models have allowed for the effects to be represented simultaneously, which represents an advance in end-to-end modelling (Travers *et al.*, 2007).

1.4. End-to-End Models

End-to-end models are models of the marine ecosystem with representation of the dynamic effects of both the physical environment and human activities on living organisms, ranging from the lowest trophic levels to the highest trophic levels (Cury *et al.*, 2008; Fennel, 2008). This approach to modelling provides a framework to understand the combined effects of fishing and climate, because it represents the whole food web and can therefore account for dynamic forcing of fishing and climate (deYoung *et al.*, 2004, Cury *et al.*, 2008).

End-to-end models can in principle be constructed by connecting biogeochemical models with fish production models. In order to achieve this connection between the model types the focus has to be on the processes which link the components of the ecosystem. The key process is predation, which affects both the growth rate of predators and the mortality of the prey (Cury *et al.*, 2008). In addition to predation other processes such as excretion can also be modelled and used to connect models of lower trophic levels with models of higher trophic levels (Megrey and Kishi, 2002; Megrey *et al.*, 2007).

Scientists working on the coupling of models are faced with a number of difficulties, which are partially caused by an increase in complexity with increasing trophic level. Organisms at higher trophic levels are more complex because they have longer life spans, more complex life histories and complex behaviours. In additions to this they also use environments with a larger spatial scale than organisms at lower trophic levels (deYoung *et al.*, 2004). The coupling is also made complicated by requiring the integration of scientific disciplines, which have very different objectives and use

different tools (Fennel, 2008; Werner *et al.*, 2007). So far, few marine models have explicitly considered the trophic links from nutrients and primary producers, up the food web, and through to fish (Werner *et al.*, 2007).

There are some models which have coupled biogeochemical models of lower trophic levels and models of higher trophic levels using biological processes (e.g. Hermann *et al.*, 2001), but they only used the predation process to achieve the connection between the models. This makes the modelled connection a one directional process, in which predation is taken as an output from the lower trophic level model and then used as an input to the higher trophic level model (Travers *et al.*, 2009).

So far only a few studies have attempted the creation of end-to-end models, by either trying to connect two already existing models or by creating a new model altogether. The model created by Travers (2009) is an example of the former. It takes ROM-N₂P₂Z₂D₂, which is a biogeochemical model connected to a hydrodynamics model, and connects it to OSMOSE, an individual based model (IBM) of multiple fish species. OSMOSE simulates the whole lifecycle of fish and represents fish schools interacting through opportunistic and size based predation on a two dimensional scale. The two models were linked through predation, which uses plankton as food available for fish and applies a mortality rate on plankton due to fish predation. It was applied to the southern Benguela ecosystem and explicitly models both environmental factors and fishing exploitation simultaneously. The output of the model showed that the two way coupling of the model improved the correspondence between simulated and observed zooplankton biomass.

Another model using the end-to-end approach is the Nemuro.fish model (Megrey *et al.*, 2007). It was constructed for the north Pacific ecosystem by linking the already existing biogeochemical model (Nemuro) with a fish population bioenergetics model. The biogeochemical model is very detailed consisting of 11 compartments with phytoplankton and zooplankton divided into 2 groups each, with three nutrient pools and one group for dissolved organic matter. The bioenergetics model for the fish simulates

the whole life cycle and have been applied to Pacific herring and saury. There are two versions of Nemuro.fish. In an uncoupled version the biogeochemical model is used as a food source but no feed back from the fish model is represented. An example for this is the application of the model to saury population off the eastern coast of Japan (Ito *et al.*, 2004). The coupled version has a feedback from the fish to the biogeochemical compartment and has been applied to herring (Megrey *et al.*, 2007). The environmental factors modelled are light and temperature in the biogeochemical department and temperature in the form of metabolic rate in the fish group. The effects of fishing are not explicitly considered.

The creation of an end-to-end model by connecting two existing models ensures that temporal and spatial scales are maintained in each part of the final model and is also more cost effective than creating completely new models (Travers *et al.*, 2007; Cury *et al.*, 2008).

One example for a model created from scratch to cover the marine environment from the nutrient up through the food web to fish is the bioenergetics model created by Fennel (2009). It represents the area of the Baltic Sea, and models three fish groups and their feeding on each other and on plankton. In the model the lower and upper trophic levels are connected via the processes of feeding and excretion. The constructed model is mass conserving apart from losses through the fishing mortality. The study used several simulations and found the model provided consistent results. In simulations with high fishing mortality the output of the model showed inter-annual variability of cod catches which resemble quantitatively the variations in data derived by multi-species stock assessment methods for the Baltic (Anonymous, 2005).

While end-to-end models allow for a better quantification of anthropogenic and climatic effects on the dynamics of marine ecosystems (Travers *et al.*, 2007), there is also a risk that the models become too complex and unfocused to be useful. Experience shows that complex models trying to represent an ecosystem as realistically as possible, rather than

representing the system with regard to a certain purpose, can be of limited use (Grimm and Railsback, 2005).

1.5. Mathematical models

In recent decades the theoretical investigation of the marine ecosystem, using mathematical models has developed into an important area of research (Fennel and Osborn, 2005). They have proven to be a good method to enable us to gain a better understanding on how the ecosystem functions and to determine which mechanisms are behind patterns in the natural world.

The advantage of simple mathematical models is that they are able to expose crucial qualitative features and their relationship to or dependence on physical processes (Truscott and Brindley, 1994). It is a good idea to use simple models for this because an increase in complexity makes it more difficult to understand model behaviour and its dependence on the model assumptions and parameters (Murray and Parslow, 1999). Mathematical models are also a useful tool because they recognize the uncertainties and shortcomings that occur with the use of observational data in models (Edwards and Brindley, 1996). They can be used to explore the model to recognise and classify the range of possible behaviours that can be expected from the system (Edwards and Brindley, 1996). These analytical properties mean that simple models can be helpful in advancing the creation of end-to-end models, because they can help to assess the relative impact of climate change and exploitation on the food web structure and dynamics, which we need to know about if we want to explore how susceptible marine ecosystems are to these processes (Frank *et al.*, 2007).

1.6. Objectives

The aim of this study was to create a simple mathematical model representing a marine ecosystem from the nutrient level up to the level of planktivorous fish. This approach allows the plankton dynamics to be linked to the fish dynamics in a simple mathematical model, which enables exploration of the dynamic behaviour of a simple end-to-end model. The results of the study will provide an idea about which dynamics need to be

included in the creation of end-to-end models. The study results will also aid in the identification of which factors have an influence on the dynamic behaviour of the model and its outputs.

2. Methods

2.1. The Models

The models used in this study are expressed in continuous time t using differential equations to describe the rates of change over time. The four state variables present in the models are: Nutrient concentration (N), Phytoplankton density (P), Zooplankton density (Z) and Fish density (F), and the flows between them are considered. The units of the state variables are mmol N/m^3 and the values for P and Z can be converted by using the constant carbon to nitrogen ratio of 6.625. The state variables are modelled using ordinary differential equations, representing a well-mixed box with no spatial structure. A schematic representation of the final model is shown in Figure 1., the model has the form of a food chain and was built up in three steps as described below. The choice of modelling a closed system was made due to the simplification affect it has on the mathematical analysis of the model. However, this simplification limits the biological interpretation of the models.

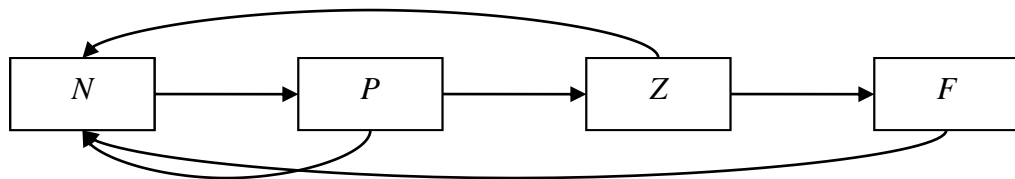


Figure 1. Schematic representation of the final NPZF model. The boxes represent the state variables and the arrows indicate the flow between them.

2.1.1. The NP Model

The first step gives the dynamics of the nutrient (N) and phytoplankton (P) as

$$\frac{dN}{dt} = \frac{-\mu NP}{N + k_n} + m_p P \quad \text{Eq 1}$$

$$\frac{dP}{dt} = \frac{\mu NP}{N + k_n} - m_p P \quad \text{Eq 2}$$

Eq. 1 describes the rate of change of nutrient concentration dN over time t . Nutrient concentration is reduced through the uptake of nutrients by phytoplankton, a type II functional response (with rate parameter μ and half saturation parameter k_n) being used to allow for saturation of uptake rate of nutrients by phytoplankton. The concentration of nutrients increases by phytoplankton instantaneously releasing nutrients when they die, which occurs at a per capita rate m_p . Eq 2 describes the rate of change of in phytoplankton density dP over time t . The rate terms here are the mirror image of those in Eq 1, so the density of phytoplankton increases by taking up nutrients, and decreases by death of phytoplankton.

In Eqs 1 and 2, a further assumption, that the total concentration of nutrients in the system $S = N + P$ is conserved, is made. We can therefore reduce the dimensions in the system by one. Eliminating the equation for nutrient dynamics leaves

$$\frac{dP}{dt} = \frac{\mu(S - P)P}{(S - P) + k_n} - m_p P \quad \text{Eq 3}$$

2.1.2. The NPZ Model

The next step adds the dynamics of the zooplankton (Z) to the system.

$$\frac{dZ}{dt} = \frac{g_z P Z \gamma_z}{P + k_p} - m_z Z \quad \text{Eq 4}$$

Eq. 4 describes the rate of change of zooplankton density (dZ) over time (t). Zooplankton density is increased through the consumption of phytoplankton, a type II functional response (with grazing rate g_z , assimilation efficiency γ_z) and half saturation parameter k_p) being used to represent a saturation per-capita ingestion rate. The unassimilated proportion of the food intake is added to the nutrient compartment. The density decreases when zooplankton dies, which occurs at the per capita rate m_z .

The addition of the zooplankton state variable results in a change of the equation describing the phytoplankton dynamics.

$$\frac{dP}{dt} = \frac{\mu(S - P - Z)P}{S - P - Z + k_n} - m_p P - \frac{g_z P Z}{P + k_p} \quad \text{Eq 5}$$

In Eq 5 a term which describes the reduction of the phytoplankton caused by zooplankton grazing is added. The constant S now represents the sum of the nutrients present in the nutrient, phytoplankton and zooplankton state variables; this means that N can be substituted for by using the expression $S = N + P + Z$.

2.1.3. The NPZF Model

In the final step a state variable representing the fish density (F) in the system was added to the model.

$$\frac{dF}{dt} = g_f ZF\gamma_f - m_f F \quad \text{Eq 6}$$

Eq. 6 describes the rate of change of fish density dF over time t . The density increases through grazing on zooplankton by fish, a type I functional response (with grazing rate g_f and assimilation efficiency γ_f) being used after the suggestion by Breck (1993) that fish are always searching for food and no saturation occurs. The population density of fish decreases at a per capita rate m_f .

This addition of the fish state variable changes the equations describing the phytoplankton and zooplankton densities of the system.

$$\frac{dP}{dt} = \frac{\mu(S - P - Z - F)P}{S - P - Z - F + k_n} - m_p P - \frac{g_z PZ}{P + k_p} \quad \text{Eq 7}$$

The phytoplankton density equation is only changed by a minimal amount because S is now $S = N + P + Z + F$

A term is added to the Zooplankton state variable to represent the reduction of its density through grazing by fish (Eq 8).

$$\frac{dZ}{dt} = \frac{g_z PZ\gamma_z}{P + k_p} - m_z Z - g_f ZF \quad \text{Eq 8}$$

2.2. Mathematical Analysis of Model Dynamics

A mathematical stability analysis was performed for each of the three models. In the process the equations of each model were analysed to obtain the equilibrium points for the model. First the locations of the equilibria were determined by solving the equations of each model simultaneously, by setting each of the differential equations describing the state variables equal to zero. Next, eigenvalue analysis was carried out to test for local stability of each equilibrium. Jacobian matrices were constructed by differentiating each equation of the model with respect to each variable, and expressions for their eigenvalues were found. The previously determined equilibria were then entered into the solution to provide the eigenvalues for our choice of parameter values. The parameter values which were used in the numerical analysis were taken from relevant literature and are shown in Table 1.

Table 1. Parameter values used in the numerical analysis of the models. Starting value concentrations (N, P, Z, F) are based on the knowledge that only around 10% of energy is transferred between trophic levels up the food chain. a Soetaert and Herman (2009) b Fennel (2009) c Christensen et al., (2000)

Parameter		Value	Unit
N	Starting value of N in numerical integrations	100	mmolN/m ³
P	Starting value of P in numerical integrations	10	mmolN/m ³
Z	Starting value of Z in numerical integrations	1	mmolN/m ³
F	Starting value of F in numerical integrations	0.1	mmolN/m ³
S	Sum of all densities present in the system		mmolN/m ³
μ	Nutrient uptake rate	0.5 ^a	day ⁻¹
γ_z	Assimilation efficiency of Z	0.7 ^a	
γ_f	Assimilation efficiency of F	0.8 ^c	
k_n	Half saturation of Nutrient	1 ^a	mmolN/m ³
k_p	Half saturation of Phytoplankton	1 ^a	mmolN/m ³
m_p	Mortality rate of Phytoplankton	0.02 ^b	day ⁻¹
m_z	Mortality rate of Zooplankton	0.05 ^a	day ⁻¹
m_f	Mortality rate of Fish	0.05 ^b	day ⁻¹
g_z	Grazing rate of Zooplankton	0.5 ^a	day ⁻¹
g_f	Grazing rate of Fish	0.005 ^b	day ⁻¹

For unstable equilibrium points at the boundary of the NP and NPZ systems a mathematical analysis was performed to check if there are any conditions under which these unstable points could be stable. This was done by applying the Routh-Hurwitz

conditions which can be used to determine if an equilibrium point is stable without having to explicitly calculate the eigenvalues (Otto and Day, 2007). The conditions are based on the values of the coefficients of the characteristic polynomials. In a two dimensional system, such as the NPZ model, the characteristic polynomial can be expressed as $r^2 + a_1r + a_2 = 0$. In order for the system to be classified as stable the conditions $a_1 > 0$ and $a_2 > 0$ have to be fulfilled simultaneously.

2.3. Phase Space Analysis

Phase space analysis was performed to gain a better understanding of the general dynamic behaviour of the models. In a phase space diagram all possible states of a system are represented, with each point in the space corresponding to a possible state, which enables general conclusions about model behaviour to be made. The phase space analysis can also be used to verify findings obtained during the mathematical analysis, to illustrate its main features with numerical examples, and to understand how the behaviour of a system will change under different parameterizations. Plotting the zero-growth isocline of each differential equation created the phase plane diagrams. Points at which isoclines intersect are equilibria. The phase plane diagram can also provide information about the stability of the equilibria. For example in a one dimensional system the stability of an equilibrium depends on the slope of the differential equation at the point. If the slope is positive i.e. to the left of the peak the equilibrium is unstable. Conversely if the slope is negative at the equilibrium i.e. to the right of the peak, the equilibrium is stable (Otto and Day, 2007).

2.4. Numerical Integrations

Numerical integrations were performed for each model to verify the findings from the previously performed analysis and to gain a better understanding of how the densities of the state variables will vary over time. The integrations were also used to see what happens to the model dynamics when starting concentrations/densities are altered. The integrations were performed using the R software package using the `odesolve` function,

which uses the 4th order Runge-Kutta integration method. The integrations were performed with step sizes which were dictated by the odesolve tolerances and accuracies. The integrations for the NP system were run from $t = 0$ to $t = 100$. For the NPZ and NPZF systems the integrations were run from $t = 0$ to $t = 1300$ to ensure the behaviour of the system was captured.

3. Results

3.1 Mathematical analysis of model dynamics

A mathematical analysis of the models was carried out to gain an understanding of the dynamics occurring in them.

3.1.1. The NP model

The mathematical analysis of the NP model showed that 2 equilibria are present in the system (Table 2). The first equilibrium was observed at $P = 0$ and the second equilibrium was observed at $\frac{\mu(S - P)}{S - P + k_n} - m_P = 0$. This equation was solved for P and on inserting the parameter values from table 1 resulted in a numerical value of $P = 109.9583 \text{ mmolN/m}^3$.

Table 2. Table showing the equilibrium points found in the NP system.

λ indicates the eigenvalues obtained in the analysis.

Equilibrium	N	P	λ
1	110	0	0.4755
2	0.0416	109.9583	-50.6688

When these points were entered into the Jacobian matrix (Eq 9) for the purpose of a stability analysis, an eigenvalue of 0.4755 was obtained for the equilibrium of $P = 0$. This means that the equilibrium is an unstable equilibrium. For the second equilibrium of $P = 109.9583 \text{ mmolN/m}^3$ an eigenvalue -50.6688 was found, which means that this equilibrium is a stable equilibrium. This means that the NP system will end up at this

state, for any biologically realistic initial condition, in which almost all of the nutrients are bound up in the phytoplankton.

The Jacobian matrix was created by differentiating the dP/dt equation shown in Eq 3 with respect to P , resulting in:

$$J = -\frac{\mu P}{S - P + k_n} + \frac{\mu(S - P)}{S - P + k_n} + \frac{\mu(S - P)P}{(S - P + k_n)^2} - m_p \quad \text{Eq 9}$$

To test for conditions in the area around the unstable equilibrium $P = 0$ can become stable the Jacobian at the point was calculated. According to the Routh-Hurwitz condition the unstable equilibrium would be stable if the condition $J(0) < 0$ is fulfilled.

$$\text{Since } J(0) = \frac{\mu S}{S + k_n} - m_p < 0 \quad \text{we can assert that } J(0) < 0 \text{ if and only if}$$

$$= \frac{\mu S}{S + k_n} < m_p.$$

This result means that at $P = 0$ the system could only be stable if the growth rate of phytoplankton is lower than its mortality rate. This means that the equilibrium could only be stable if the phytoplankton population is going extinct.

3.1.2. The NPZ Model

After the addition of the differential equation defining the zooplankton state variable as shown in equation 4, the mathematical analysis was repeated. The results showed the presence of three equilibria in the NPZ system (Table 3).

The equilibrium value of P was obtained by setting $dZ/dt = 0$ in equation 4. This is true

$$\text{if } Z = 0 \text{ or if } \frac{g_z P \gamma_z}{P + k_p} - m_z = 0. \text{ This can be expressed as } P = \frac{m_z k_p}{g_z \gamma_z - m_z}. \text{ Inserting}$$

the parameter values from table 1 into this term, a value of $P^* = 0.1667 \text{ mmolN/m}^3$ was obtained.

Next, setting $dP/dt = 0$ in equation 5 yields two possible solutions: $P = 0$ or $\frac{\mu(S - P - Z)}{S - P - Z + k_n} - m_p - \frac{g_z Z}{P + k_p} = 0$. When the second equation was solved under the assumption that $P = P^*$, one positive solution for Z was obtained. When parameter values from table 1 were inserted into this solution a numerical value of $Z = 1.109463 \text{ mmolN/m}^3$ was obtained.

If $dP/dt = 0$ is solved under the assumption that $Z = 0$ the equation is reduced to the equation $\frac{\mu(S - P)P}{S - P + k_n} - m_p P = 0$, which has two possible solutions. These are at $P = 0$

and $\frac{\mu(S - P)}{S - P + k_n} - m_p = 0$, i.e. $P = 0$ or $P = \frac{-\mu S + m_p S + m_p k_n}{m_p - \mu}$. When parameter

values from table 1 were entered into this second solution a value of $P = 110.9583 \text{ mmolN/m}^3$ was obtained. This gives three equilibria as shown in table 3. The values are slightly different to the values in table 2 due to the addition of the zooplankton state variable to the system. This means the value of S is increased to $S = 111$ from the previous value of $S = 110$.

Table 3. Table showing the equilibrium points found in the NPZ system.

λ indicates the eigenvalues obtained in the analysis

Equilibrium	N	P	Z	λ_1	λ_2
1	111	0	0	0.4755357	-0.05
2	0.0416667	110.9583	0	-51.1296	0.2968738
3	109.7239	0.16667	1.109963	0.0339+0.139i	0.0339-0.139i

As with the NP model in section 3.1.1. these results were entered into the Jacobian matrix (Eq 10) of the system and used in an eigenvalue analysis. The Jacobian matrix is defined as

$$J = \begin{pmatrix} \frac{\partial \frac{dP}{dt}}{\partial P} & \frac{\partial \frac{dP}{dt}}{\partial Z} \\ \frac{\partial \frac{dZ}{dt}}{\partial P} & \frac{\partial \frac{dZ}{dt}}{\partial Z} \end{pmatrix}. \quad \text{Eq 10}$$

The elements of the first row are comprised by differentiating the dP/dt equation as shown in equation 5, with respect to P and Z , resulting in

$$\frac{\partial \frac{dP}{dt}}{\partial P} = -\frac{\mu P}{S-P-Z+k_n} + \frac{\mu(S-P-Z)}{S-P-Z+k_n} + \frac{\mu(S-P-Z)P}{(S-P-Z+kn)^2} - m_p - \frac{g_z Z}{P+k_p} + \frac{g_z PZ}{(P+k_p)^2}$$

and

$$\frac{\partial \frac{dP}{dt}}{\partial Z} = -\frac{\mu P}{S-P-Z+k_n} + \frac{\mu(S-P-Z)P}{(S-P-Z+k_n)^2} - \frac{g_z P}{P+k_p}$$

respectively. The elements of the second row were created by differentiating the dZ/dt differential equation as shown in equation 4, with respect to P and Z resulting in

$$\frac{\partial \frac{dZ}{dt}}{\partial P} = \frac{g_z Z \gamma_z}{P+k_p} - \frac{g_z PZ \gamma_z}{(P+k_p)^2}$$

and

$$\frac{\partial \frac{dZ}{dt}}{\partial Z} = \frac{g_z P \gamma_z}{P+k_p} - m_z$$

respectively. The explanations and values of parameters used can be found in Table 1.

The results of this stability analysis of the system showed that all equilibria within the systems are unstable equilibria. In addition to this the analysis showed that the equilibrium point where N , P and Z coexist, is classified as an unstable focus in the system. This is indicated by the eigenvalues, which are complex numbers with a positive real part (Table 3). The positive value indicates instability and the complex number indicates the equilibrium is a focus.

When applying the Routh-Hurwitz conditions of stability to the NPZ system the following results were obtained. In the area around equilibrium 1 the Routh-Hurwitz conditions would only be fulfilled if the phytoplankton density is declining. In the area around equilibrium 2 the Routh-Hurwitz conditions are only fulfilled if both the phytoplankton and zooplankton densities are in decline.

3.1.3. The NPZF Model

As in section 3.1.1. and 3.1.2. the mathematical analysis was repeated after the addition of the differential equation, which in this case describes the fish state variable as shown in equation 6. The analysis of the NPZF model showed that five equilibria are present in the system. Two out of these were found to be internal equilibria and the three remaining equilibria are located on the boundaries of the system.

The first step to determine the equilibria in the system was to set $dF/dt = 0$ in equation 6. This has the solutions $F = 0$ and $g_f Z \gamma_f - m_f = 0$. This second equation can be expressed

as $Z = \frac{m_f}{g_f \gamma_f}$. Inserting the parameter values from table 1 into this equation for Z gives

an equilibrium value of $Z = 12.5 \text{ mmolN/m}^3$.

Next the equation $dZ/dt = 0$ in equation 8 was solved resulting in two solutions. The first

is given by $Z = 0$ and the second is given by $\frac{g_z P \gamma_z}{P + k_p} - g_z F - m_z = 0$. When this

equation is solved for F it can be expressed as $F = \frac{g_z P \gamma_z - m_z P - m_z k_p}{(P + k_p) g_f}$.

Finally there are also two possible solutions for $dP/dt = 0$ in equation 7, the first being

$P = 0$ and the second being $\frac{\mu(S - P - Z - F)}{S - P - Z - F + k_n} - m_p - \frac{g_z Z}{P + k_p} = 0$. This second

solution can also be expressed as

$$F = \frac{(\mu SP - \mu Sk_p - \mu P^2 - \mu Pk_p - \mu ZP - \mu Zk_p + m_p Pk_p + m_p Zk_p - g_z ZS + g_z ZP + g_z Z^2}{(-g_z Z - m_p P + \mu P + \mu k_p - m_p k_p)} \\ + \frac{m_p ZP - g_z Zk_n - m_p SP + m_p P^2 - m_p Pk_n - m_p Sk_p - m_p k_p k_n}{}$$

Because the equations defining F resulting from solving the dP/dt and the dZ/dt equations can only be defined as a function of P , a slightly different approach had to be employed to obtain a solution for F that is “independent” of P and vice versa.

To obtain a solution for P independent of F , the solutions obtained for F from the dZ/dt and the dP/dt equations were set equal to each other and then solved for P . The solution had the shape of a cubic equation, which resulted in one negative, and two positive values for P when the parameter values from table 1 were inserted into the solution. The positive values were 12.45406 mmolN/m³ and 39.78610 mmolN/m³. Inserting these obtained values of P into the solutions for F the results were 54.79711 mmolN/m³ and 58.28373 mmolN/m³ respectively. This gives the five equilibria as shown in table 4. Again the values are slightly different to the values in table 2 and 3 due to the addition of the fish state variable to the system. This means the value of S is increased to $S = 111.1$ from the previous value of $S = 111$.

Table 4. Table showing the equilibrium points found in the NPZF system.

λ indicates the eigenvalues obtained in the analysis

Equilibrium	N	P	Z	F	λ_1	λ_2	λ_3
1	111.1	0	0	0	0.4755	-0.05	-0.05
2	0.0416	111.058	0	0	-51.172	0.2968	-0.05
3	109.777	0.166	1.156	0	-0.0454	0.0255+0.1419i	0.0255-0.1419i
4	31.348	12.454	12.5	54.797	0.3977	0.0132+0.1198i	0.0132-0.1198i
5	0.53	39.786	12.5	58.283	-8.2439	-0.0014+0.124i	-0.0014-0.124i

When these obtained values were inserted into the Jacobian matrix (Eq 11) of the system and used in an eigenvalue analysis the result showed that out of the two internal equilibria one, equilibrium 4, was found to be unstable and the other, equilibrium 5, was found to be stable, the former having a lower density of fish than the latter. The

eigenvalues obtained from the eigenvalue analysis are shown in table 4. The Jacobian matrix is defined as

$$J = \begin{pmatrix} \frac{\partial \frac{dP}{dt}}{\partial P} & \frac{\partial \frac{dP}{dt}}{\partial Z} & \frac{\partial \frac{dP}{dt}}{\partial F} \\ \frac{\partial \frac{dZ}{dt}}{\partial P} & \frac{\partial \frac{dZ}{dt}}{\partial Z} & \frac{\partial \frac{dZ}{dt}}{\partial F} \\ \frac{\partial \frac{dF}{dt}}{\partial P} & \frac{\partial \frac{dF}{dt}}{\partial Z} & \frac{\partial \frac{dF}{dt}}{\partial F} \end{pmatrix}. \quad \text{Eq 11}$$

The elements of the first row are comprised by differentiating the dP/dt differential equation as shown in equation 7 with respect to P , Z and F resulting in:

$$\frac{\partial \frac{dP}{dt}}{\partial P} = -\frac{\mu P}{S-P-Z-F+k_n} + \frac{\mu(S-P-Z-F)}{S-P-Z-F+k_n} + \frac{\mu(S-P-Z-F)P}{(S-P-Z-F+k_n)^2} - m_p - \frac{g_z Z}{P+k_p} + \frac{g_z PZ}{(P+k_p)^2},$$

$$\frac{\partial \frac{dP}{dt}}{\partial Z} = -\frac{\mu P}{S-P-Z-F+k_n} + \frac{\mu(S-P-Z-F)P}{(S-P-Z-F+k_n)^2} - \frac{g_z P}{P+k_p}$$

and

$$\frac{\partial \frac{dP}{dt}}{\partial F} = -\frac{\mu P}{S-P-Z-F+k_n} + \frac{\mu(S-P-Z-F)P}{(S-P-Z-F+k_n)^2}$$

respectively. The elements of the second row were created by differentiating the dZ/dt differential equation as shown in equation 8 with respect to P , Z and F resulting in

$$\frac{\partial \frac{dZ}{dt}}{\partial P} = \frac{g_z Z \gamma_z}{P+k_p} - \frac{g_z PZ \gamma_z}{(P+k_p)^2},$$

$$\frac{\partial \frac{dZ}{dt}}{\partial Z} = \frac{g_z P \gamma_z}{P+k_p} - g_f F - m_z$$

and

$$\frac{\partial \frac{dZ}{dt}}{\partial F} = -g f Z$$

respectively. Finally the third row of the matrix is created by differentiating the dF/dt differential equation as shown in equation 6 with respect to P , Z and F resulting in

$$\frac{\partial \frac{dF}{dt}}{\partial P} = 0,$$

$$\frac{\partial \frac{dF}{dt}}{\partial Z} = g f F \gamma f$$

and

$$\frac{\partial \frac{dF}{dt}}{\partial F} = g f Z \gamma z - m f$$

respectively.

3.2. Phase space analysis

The phase space analyses of the three models were performed to gain a better understanding of the general behaviour of the models and to give support to the results obtained during the mathematical analysis. To make the diagrams easier to understand only the internal zero-growth isoclines will be displayed in the diagrams below.

3.2.1. The NP model

To create the phase plane diagram for the NP model the zero-growth isocline were calculated. In the NP system, two such zero-growth isoclines were identified (Figure 2). The first is at $P = 0$ and the second at $\mu(S - P) - m_p S + m_p P - m_p k_n = 0$. To the left of the equilibrium the density of phytoplankton is increasing while to the right of the equilibrium the phytoplankton density is decreasing.

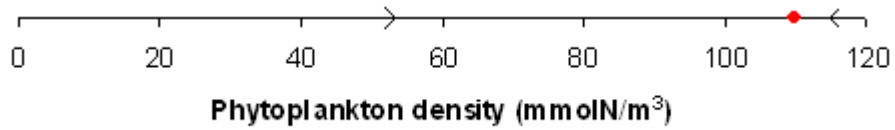


Figure 2. Graph showing the equilibrium of the NP system. The Red dot shows the position of the equilibrium. The arrows indicate the direction of the trajectories in the system.

The results from the phase space analysis verify the mathematical analysis of the system with regards to the position of the equilibrium found in the system.

3.2.2. The NPZ model

The addition of the differential equation 4, which describes the zooplankton state variable, resulted in the addition of two additional zero-growth isocline to the system.

Each of the two differential equations used to describe the system results in a boundary and an internal zero-growth isocline (Figure 3). The dP/dt differential equation as shown in equation 5 has a zero-growth isocline at $P = 0$ and at

$$\frac{\mu(S - P - Z)}{S - P - Z + k_n} - m_p - \frac{g_z Z}{P + k_p} = 0.$$

The dZ/dt differential equation as shown in equation 4 has one zero-growth isocline at $Z = 0$ and another one at $\frac{g_z P \gamma_z}{P + k_p} - m_z = 0.$

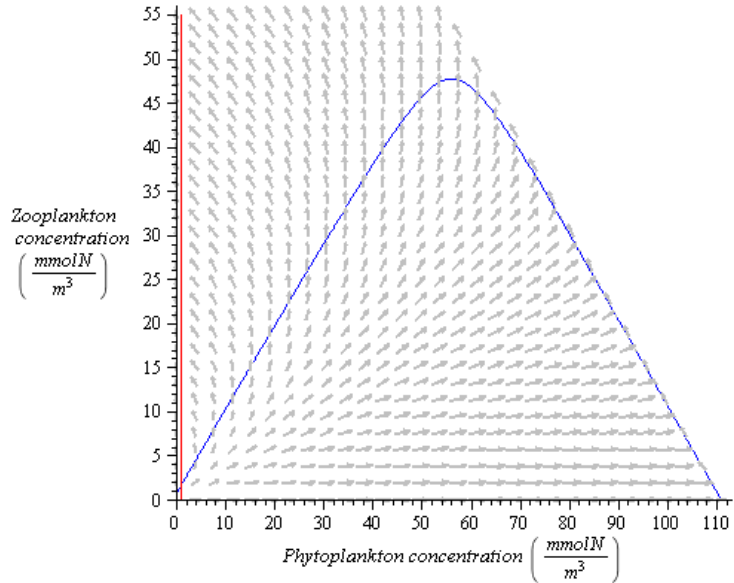


Figure 3. Phase space portrait of the NPZ system. The blue line shows the internal zero growth isocline of phytoplankton equation 5. The red line shows the internal zero-growth isocline of zooplankton equation 4. The grey arrows are the vector field of the system. The internal equilibrium is situated at the intersection of the two internal zero-growth isoclines.

A magnification of the phase space area around the internal equilibrium shows that the trajectories move in circle spiraling out from the equilibrium (Figure 4).

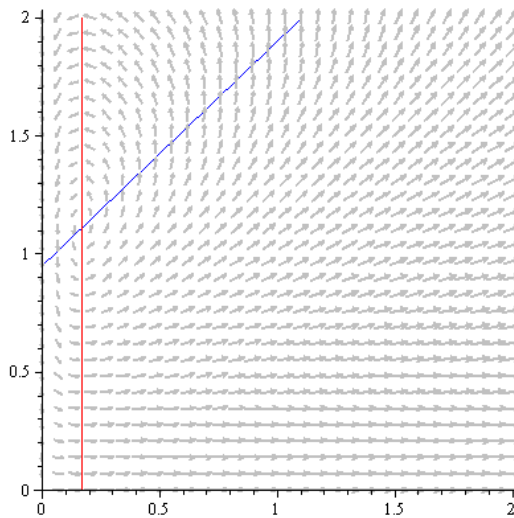


Figure 4. Magnification of the area from 0 to 2 of the NPZ Phase space portrait. The blue line shows the internal zero growth isocline of phytoplankton equation 5 . The red line shows the internal zero-growth isocline of zooplankton equation 4. The grey arrows are the vector field of the system. The internal equilibrium is situated at the intersection of the two internal zero-growth isoclines.

The two internal zero-growth isocline effectively divide the phase space into four areas, with the density of phytoplankton is increasing beneath the blue curve and decreasing above it. The zooplankton density is decreasing to the left of the red line and increasing to the right of it.

In the first area located in the bottom left of the diagram the zooplankton density is decreasing while the phytoplankton density is increasing. In the second area in the bottom right the phytoplankton and zooplankton densities are both increasing. In the third area in the top right the phytoplankton density is decreasing while the zooplankton density is increasing. In the top left, the fourth area, to the left of the zooplankton and above the phytoplankton zero-growth isoclines, both the zooplankton and the phytoplankton densities are decreasing.

The results obtained from the phase space analysis verify the results from the mathematical analysis with regards to the position of the equilibria in the system. The phase space and the mathematical analysis both indicated the presence of a stable limit cycle in the system. Following the Poincare-Bendixon theorem a stable limit cycle has to be present because there is no attracting fixed point present in the system and it is a two-dimensional system (see Edelstein-Keshet, 1988).

The position of the internal equilibrium is defined by the equation $\frac{g_z P \gamma_z}{P + k_p} - m_z = 0$.

The isocline would shift towards the right either if the zooplankton mortality is increasing or if the zooplankton growth rate is decreasing (Figure 5).

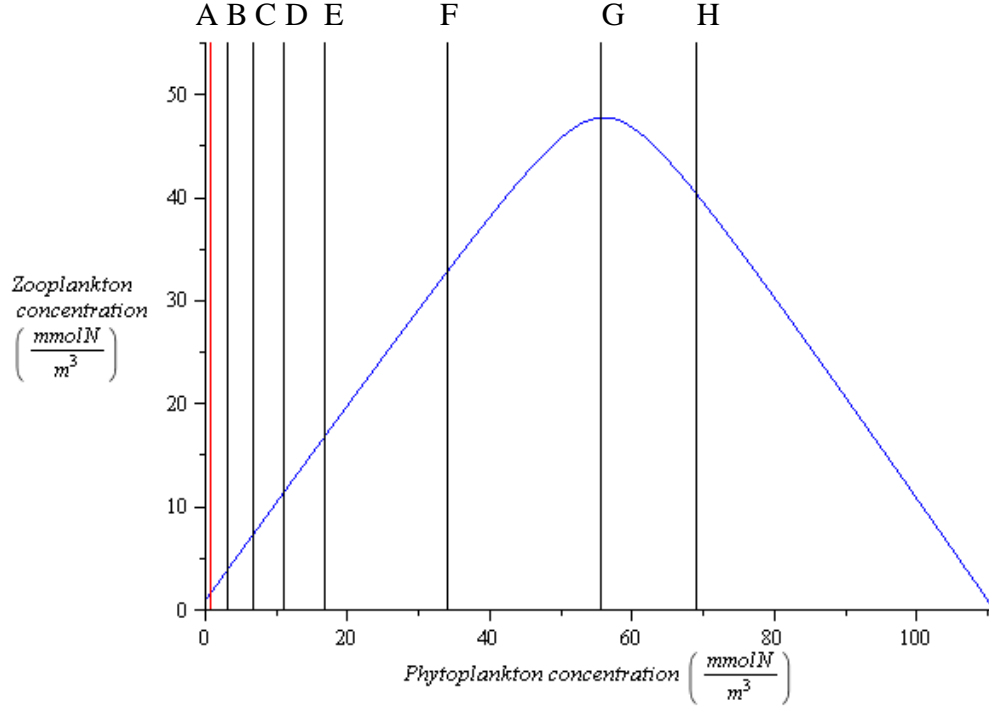


Figure 5. Shift of the internal zooplankton zero-growth isocline. Figure shows the different positions of the internal zooplankton zero-growth isocline with increasing values of m_z . A: $m_z = 0.05$, B: $m_z = 0.2$, C: $m_z = 0.3$, D: $m_z = 0.32$, E: $m_z = 0.33$, F: $m_z = 0.34$, G: $m_z = 0.3438$, H: $m_z = 0.345$

3.2.3. The NPZF model

With the addition of the differential equation 6, which describes the fish state variable of the system, a third internal zero-growth isocline was added to the system. The zero-growth isoclines for dF/dt equation 6 were observed to be at $F = 0$ and at $Z = \frac{m_f}{g_f \gamma_f}$.

This means that the internal zero-growth isocline which is obtained from the dF/dt differential equation is a constant with the value of $Z = 12.5 \text{ mmol/m}^3$. The curves of the dZ/dt equation as shown in equation 8 are at $Z = 0$ or $F = \frac{g_z P \gamma_z - m_z P - m_z k_p}{(P + k_p) g_f}$.

The zero-growth isoclines of the dP/dt differential equation as shown in equations 7 are at $P = 0$ and at $\frac{\mu(S - P - Z - F)}{S - P - Z - F + k_n} - m_p - \frac{g_z Z}{P + k_p} = 0$.

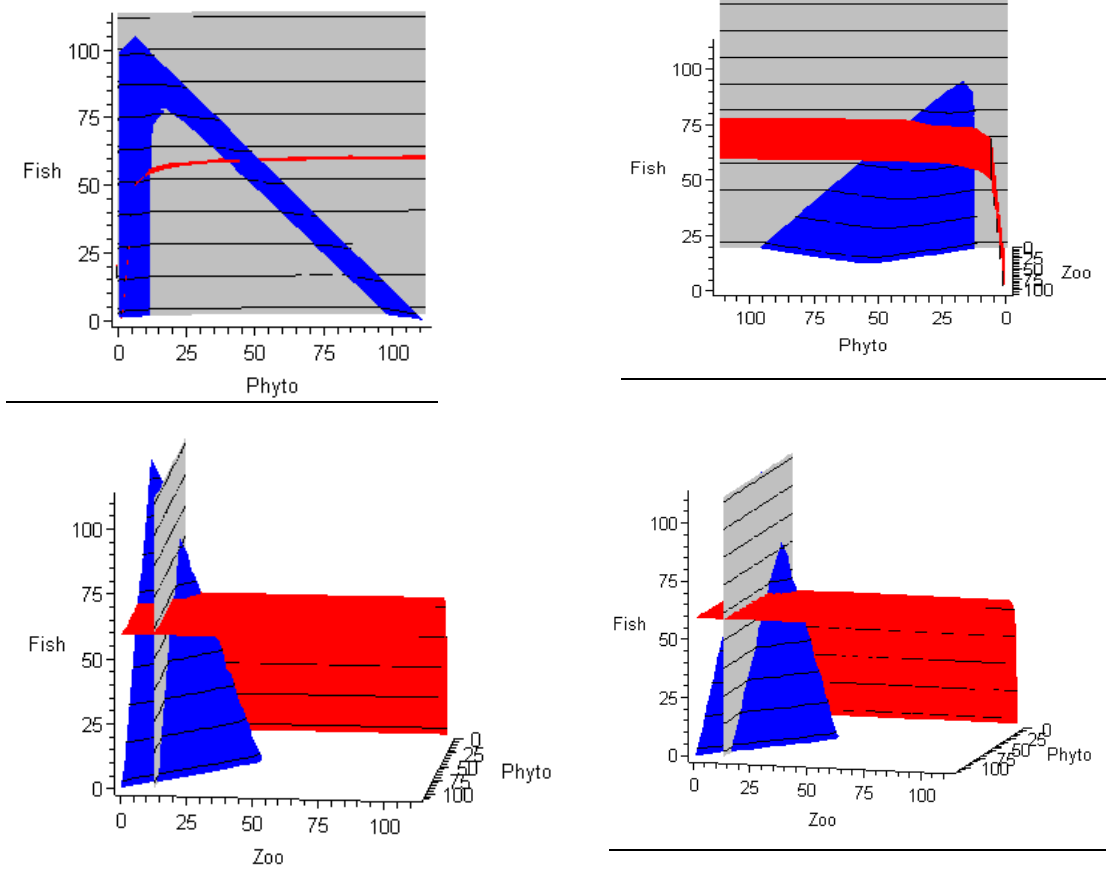


Figure 6. Different views of the internal zero-growth isocline surfaces of the NPZF model. Blue is the internal zero-growth isocline for phytoplankton, red is the zero growth isocline for zooplankton and grey is the zero-growth isocline for zooplankton. Equilibria are located at the intersection of all three surfaces.

In the phase space diagram (Figure 6) the internal zero-growth isoclines divide the phase space into eight areas based on the following conditions. The phytoplankton densities are increasing beneath the blue dome shape and decreasing outside it. The zooplankton densities are increasing below the red surface and decreasing below it. The fish densities are increasing behind the grey surface, and decreasing in front of it.

This means that in the area which is located behind the grey surface, beneath the red plane and inside the blue dome shape the densities of all three functional groups are increasing. In the area which is under the red plane but outside, the blue dome shape the phytoplankton density is decreasing while the zooplankton and fish densities are increasing. Above the red surface and inside the blue dome shape the densities of phytoplankton and fish are increasing while the density of zooplankton is decreasing. In the region outside the blue dome shape both phytoplankton and zooplankton densities

are decreasing and only the fish density is increasing. In the area, which is lying in front of the fish zero-growth isocline, the densities are behaving in the following ways. Beneath the red surface and inside the blue dome shape the densities for the phytoplankton and zooplankton state variable are increasing while the fish density is decreasing. Outside the blue dome shape the concentrations of the phytoplankton and fish groups are decreasing with only the zooplankton concentration increasing. Above the red surface and inside the blue dome shape only the phytoplankton density is increasing while both the zooplankton and fish densities are decreasing. In the area above the red surface and outside the blue dome all three densities are decreasing.

On introduction of the fish state variable the phytoplankton zero-growth isocline remained unaffected, while the zooplankton zero-growth isocline was observed to bend towards the right. This is the case because the fish only have direct influence on the zooplankton state variable by preying on them while they do not prey on the phytoplankton.

The position of the internal equilibrium points is determined by the internal fish zero-growth isocline, which is defined by the equation $Z = \frac{m_f}{g_f \gamma_f}$. The plane would move

backward in the space either if the mortality of fish is increasing or if the growth rate of fish decreases. If the surface is shifted sufficiently far back in the space, it will no longer intersect the two remaining zero-growth isocline surfaces present in the system (Figure 7). This means that a change in the fish mortality parameter value can cause a bifurcation.

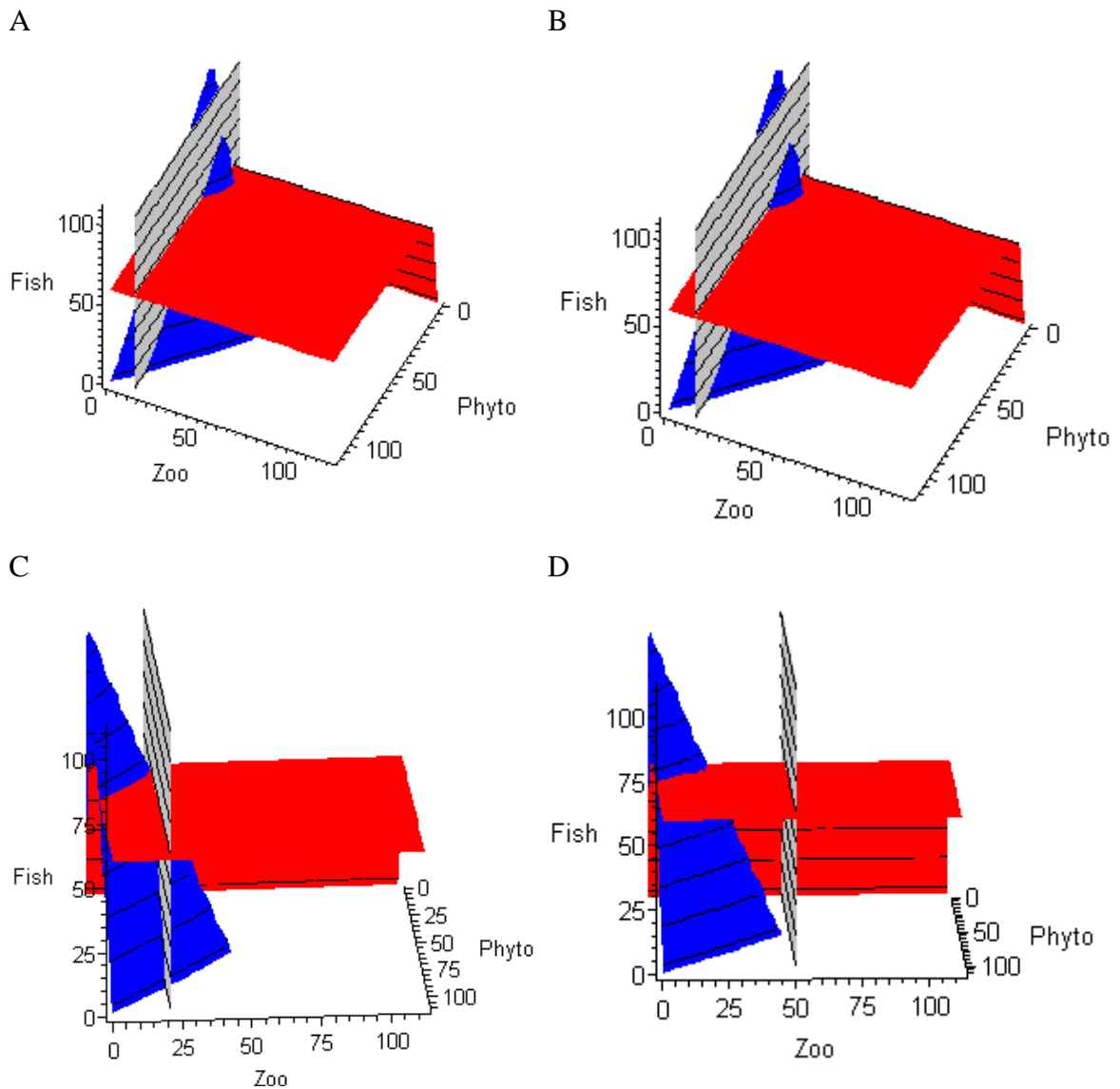


Figure 7. Shift of the internal Fish zero-growth isocline. Figure showing different positions of the fish zero-growth isocline for increasing m_f values. A: $m_f = 0.05$, B: $m_f = 0.07$, C: $m_f = 0.83$, D: $m_f = 0.2$

3.3 Numerical Integrations

3.3.1. The NP model

The numerical integration of the NP system (Figure 8) was performed using the `odesolve` function in the R software package, which uses the 4th order Runge-Kutta method, from $t = 0$ to $t = 100$ with a step size of 1 day. The graphical result shows that the nutrient concentration is rapidly taken up during an increase in the phytoplankton

density. The phytoplankton density can be observed to level when it reaches a value of around $109.9583 \text{ mmolN/m}^3$. This behaviour observed in the numerical integration verifies the results from the mathematical analysis of the NP model, which indicated a stable equilibrium at this value of phytoplankton density.

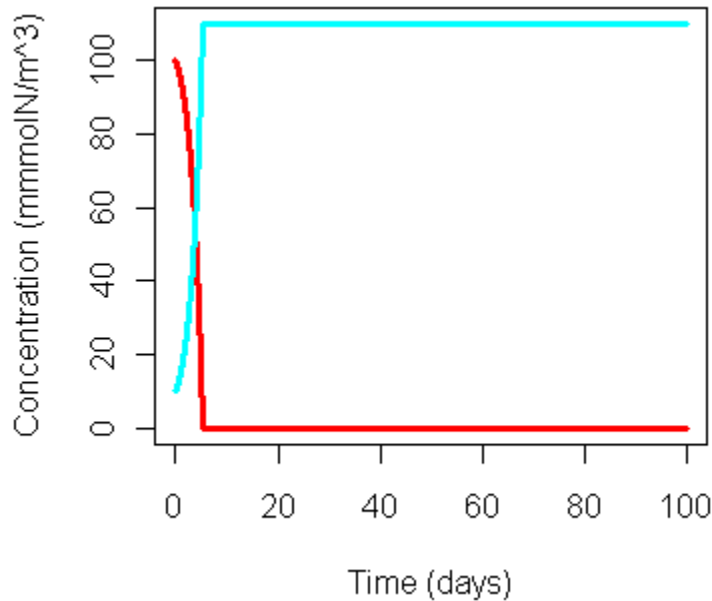


Figure 8. Graph of the numerical integration of the NP system. Red is the nutrient concentration, blue is the phytoplankton density.

3.1.2. The NPZ model

As in section 3.1.1. the numerical integration of the NPZ model was performed using the `odesolve` function in the R software package, which uses the 4th order Runge-Kutta method, from $t = 0$ to $t = 1300$ at a step size of 1 day. The graphical result shows a limit cycle in the densities of the functional groups present in the system (Figure 9). The observed behaviour of the densities is the following: As the phytoplankton density increases the nutrient concentration declines. Then as the zooplankton density increases the phytoplankton density declines. When the zooplankton density declines the nutrient concentration increases again, before the cycle restarts with an increase in phytoplankton density.

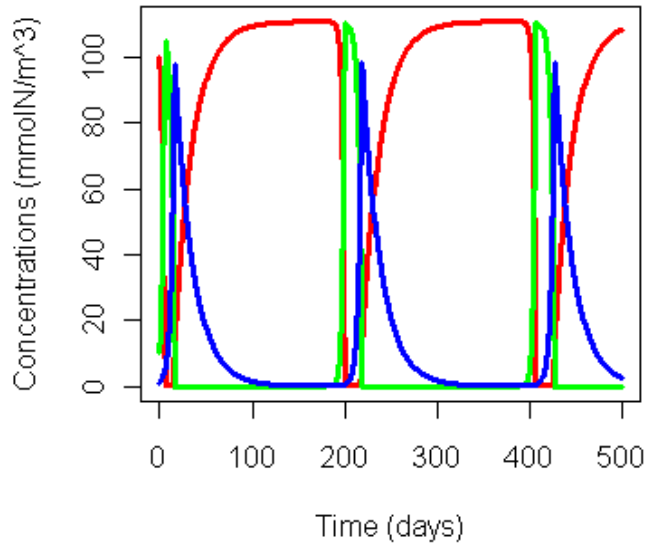


Figure 9. Graph of numerical integration of the NPZ system. Red shows the nutrient concentration and green and blue represent the phytoplankton and zooplankton densities respectively.

When the results of the numerical integrations were plotted into phase space it was observed that independent of the starting values the trajectories move into the limit cycle. This suggests a stable limit cycle (Figure 10). In the third panel of figure ten the trajectory is approaching the limit cycle.

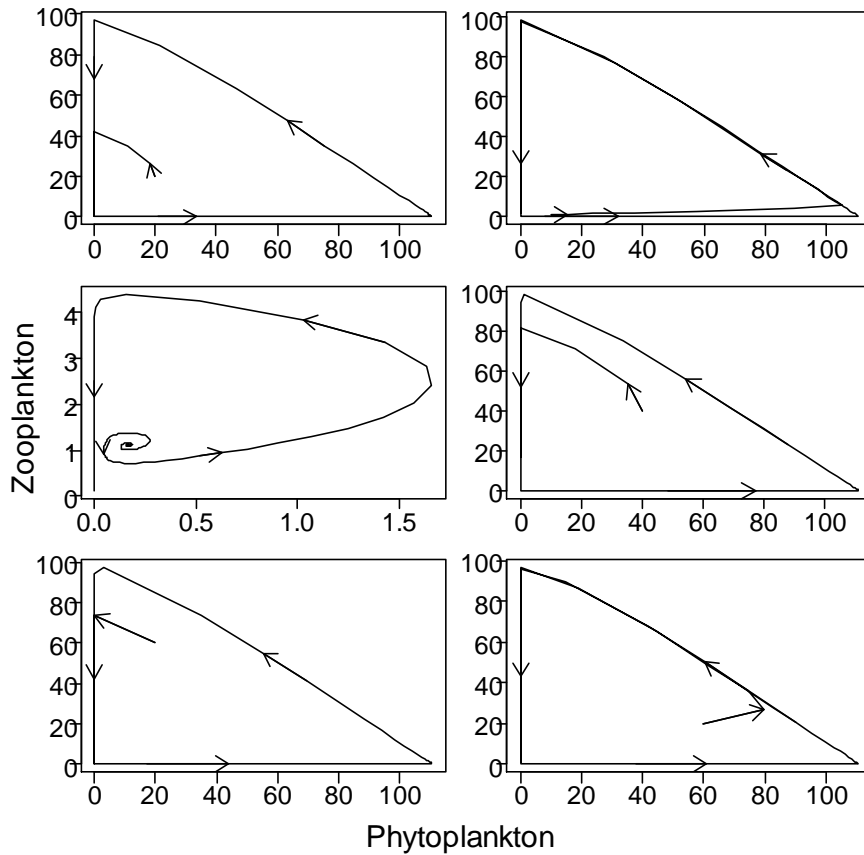


Figure 10. Phase space portrait of the NPZ system. Showing trajectories from different starting points in the system. The units for both phytoplankton and zooplankton densities are mmolN/m^3

The observations from the numerical integrations verify the results which were obtained during the phase space analysis using equations 3 and 4 of the model in section 3.2.2.. The behaviour of the integration in which the phytoplankton density increases while the density of zooplankton decreases corresponds to the first area in the phase space diagram. The part of the integration in which both the phytoplankton and zooplankton densities are increasing simultaneously can be assigned to the second area in the phase space diagram, while the area with decreasing phytoplankton and increasing zooplankton densities corresponds to the third area in the phase space diagram. The last part of the cycle in which both the phytoplankton and zooplankton densities are observed to decrease relates to the fourth area on the phase space diagram.

3.3.3. NPZF model

As in the two previous models in sections 3.3.1. and 3.3.2. numerical integrations were performed using the `odesolve` function in the R software package, which uses the 4th order Runge-Kutta method, for the NPZF model. The integration of the model was run from $t = 0$ to $t = 1300$ at a step size of 1 day. The numerical integrations revealed two areas of behaviour in the system, indicating bistability with a basin boundary being present.

In the first area, with a value in fish density above the boundary value, the behaviour that can be observed in the integration is that the densities of nutrient, phytoplankton, zooplankton and fish are oscillating towards the stable equilibrium in the system (Figure 11). This behaviour was expected to occur based on the mathematical analysis of the equations 6, 7 and 8 of the NPZF model in section 3.1.3..

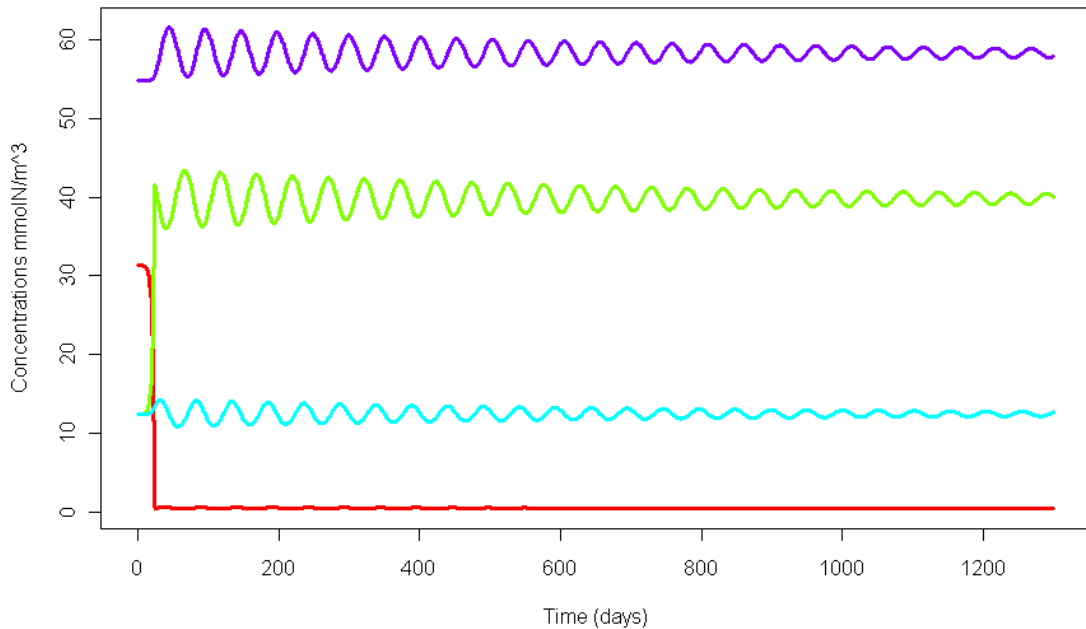


Figure 11. Result of the numerical integration in NPZF system with starting value slightly higher than the value of the unstable internal equilibrium point of the system. Red shows the nutrient concentration and green, turquoise and purple represent the phytoplankton, zooplankton and fish densities respectively

This behaviour can be observed as a spiraling towards the stable equilibrium in the system when the results obtained from the numerical integrations are plotted into the phase space of the system (Figure 12).

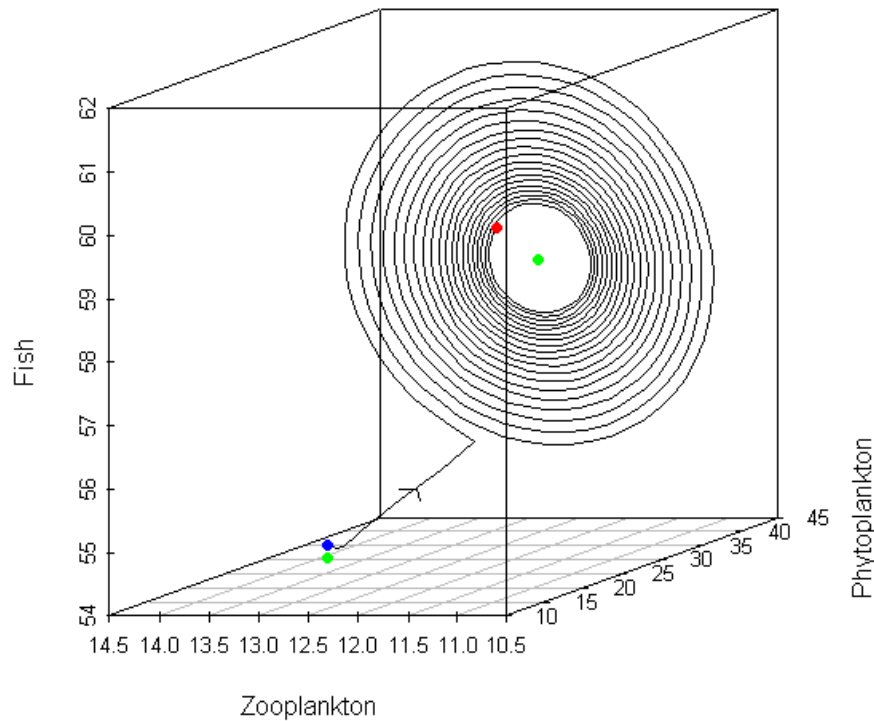


Figure 12. Phase space portrait of the numerical integrations shown in figure 11.

Blue dot represents starting point of the integration, red dot represents end point of the integration, green dots indicate the position of the equilibrium points. Arrows indicate the direction of the movement of the integration. The units for both phytoplankton, zooplankton and fish densities are mmolN/m^3

In the second area of behaviour that has been observed in the system, the fish density occurring in the system tends towards zero after initial cycling, leaving only the nutrient concentration and phytoplankton and zooplankton densities to continue to cycle. The slow spiraling of the trajectories towards the equilibrium and the closeness to zero of the real parts of the complex eigenvalues for equilibrium 5 in Table 4, indicates that the equilibrium is close to going through Hopf bifurcation.

When the integrations were run with the initial starting conditions shown in table 1 the graphical result shows the densities of the state variables going through one increase phase before declining again (Figure 13). The only state variable having the opposite behaviour is the nutrient concentration. After one cycle including all four state variables, only the nutrient, phytoplankton and zooplankton densities continue cycling as is the NPZ system.

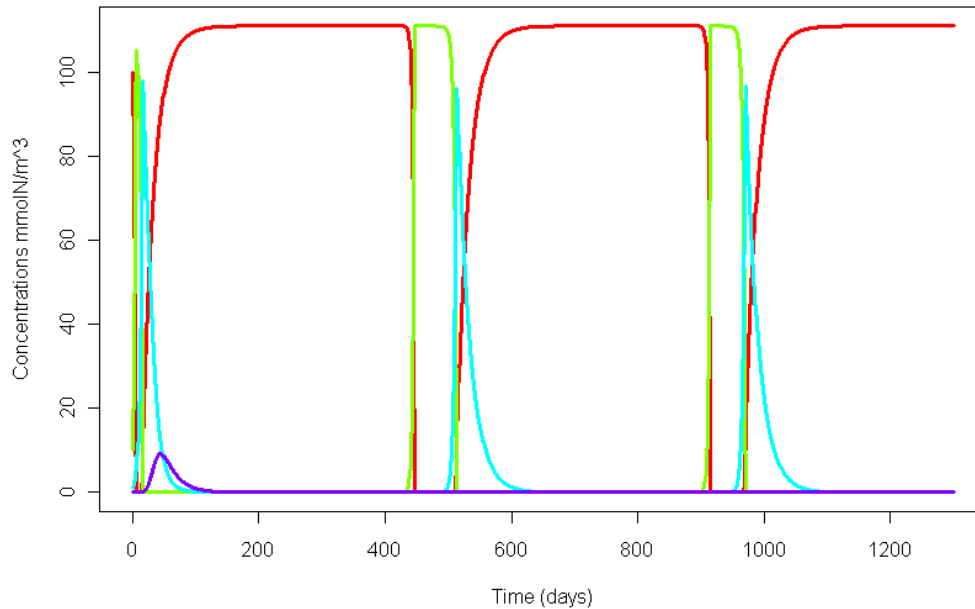


Figure 13. Numerical integration of the NPZF system Red shows the nutrient concentration and green, turquoise and purple represent the phytoplankton, zooplankton and fish densities respectively

When the result from the numerical integrations was plotted in the phase space this behaviour was also observed, represented as cycles in the bottom plane (Figure 14).

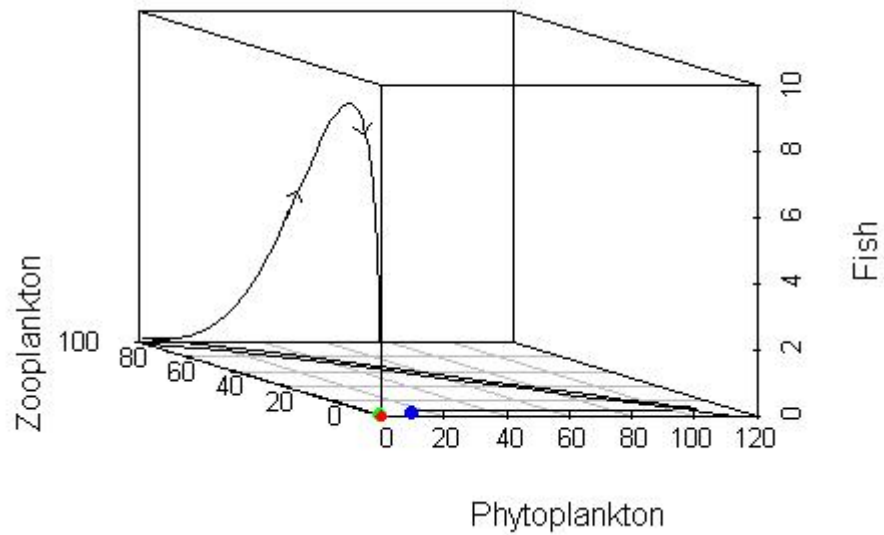


Figure 14. Phase space portrait of the numerical integrations shown in figure 13.

Blue dot represents starting point of the integration, red dot represents end point of the integration, green dot indicates the position of the equilibrium. Arrows indicate the direction of the movement of the integration. The units for both phytoplankton, zooplankton and fish densities are mmolN/m^3

The result was also observed when integrations were started at the values of $F = 54.797$ mmolN/m^3 , $P = 12.454$ mmolN/m^3 and $Z = 12.5$ mmolN/m^3 , the value at the unstable equilibrium. After the initial cycle the behaviour was similar to the ones observed during the initial integration for the model (Figure 15).

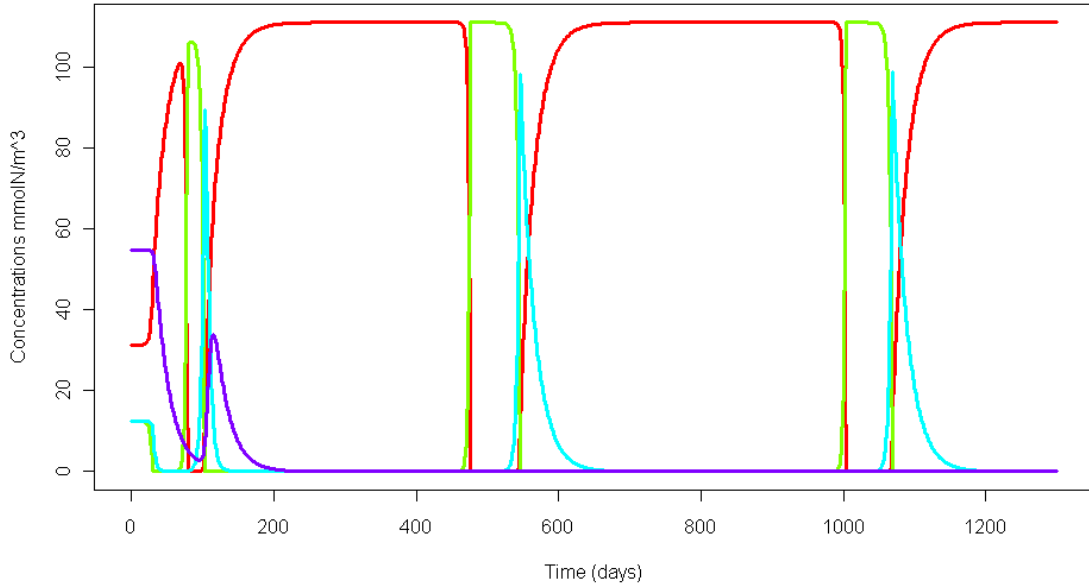


Figure 15. Result of the numerical integration in NPZF system with starting value represented at the unstable internal equilibrium point of the system Red shows the nutrient concentration and green, turquoise and purple represent the phytoplankton, zooplankton and fish densities respectively

As before the results of the numerical integrations were plotted in the phase space of the system (Figure 16).

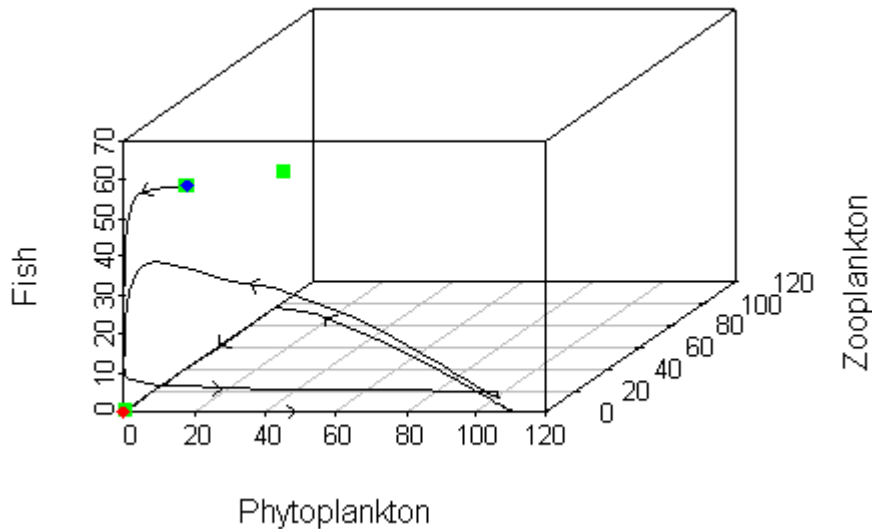


Figure 16. Phase space portrait of the numerical integrations shown in figure 15. Blue dot represents starting point of the integration, red dot represents end point of the integration, green dots indicate the position of the equilibria. Arrows indicate the direction of the movement of the integration. The units for both phytoplankton, zooplankton and fish densities are mmolN/m^3

When the value of the fish density was increased to $F = 130 \text{ mmolN/m}^3$ the behaviour observed in the graphical result of the numerical integrations also showed a settling of the densities into a cycle in the nutrient, phytoplankton and zooplankton densities (Figure 17).

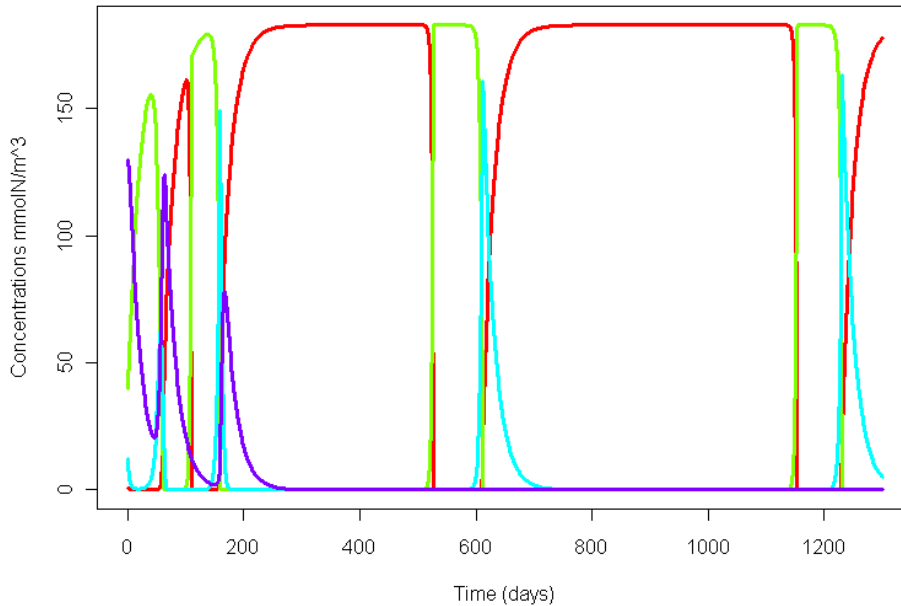


Figure 17. Result of the numerical integration in NPZF system with a starting value of $F = 130 \text{ mmolN/m}^3$ at the values of the stable internal equilibrium point of the system Red shows the nutrient concentration and green, turquoise and purple represent the phytoplankton, zooplankton and fish densities respectively

The same behaviour can also be observed when the integration results are plotted into the phase space of the system (Figure 18).

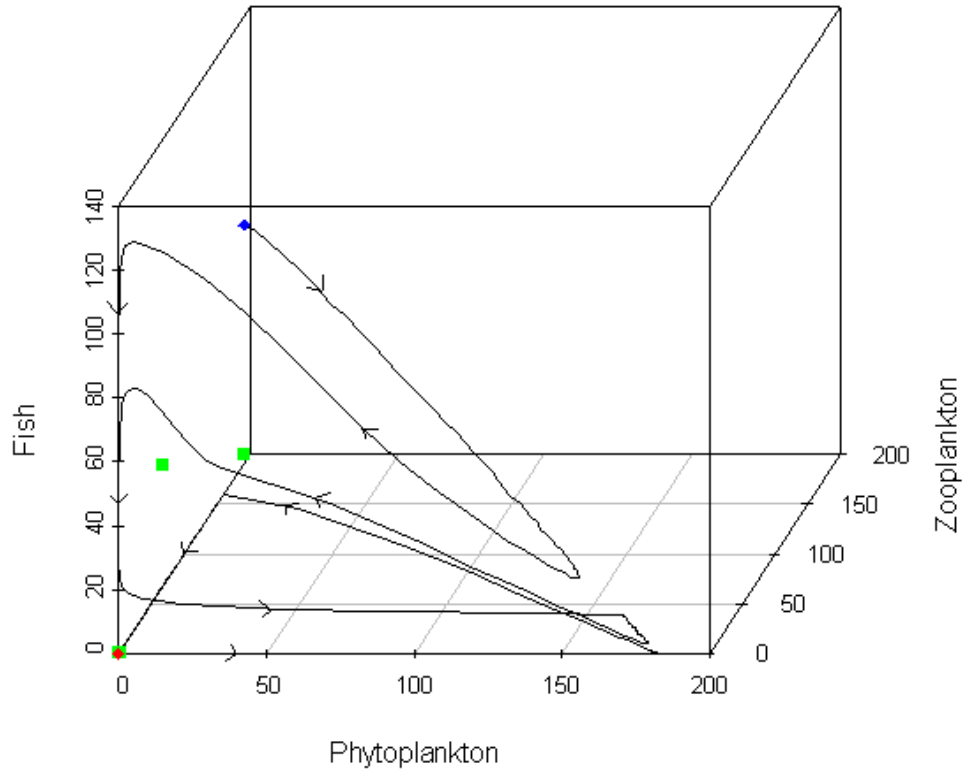


Figure 18. Phase space portrait of the numerical integrations shown in figure 17. Blue dot represents starting point of the integration, red dot represents end point of the integration, green dots indicate the position of the equilibrium points. Arrows indicate the direction of the movement of the integration. The unites for both Phytoplankton, Zooplankton and Fish densities are mmolN/m^3

4. Discussion

4.1. The NP model

In the system in which only nutrients and phytoplankton occur, the system was found to be stable in a state in which most nutrients have been taken up by the phytoplankton. The behaviour change in the system was observed to be rapid, with the phytoplankton taking up the nutrients present in the system before levelling. The levelling in the phytoplankton density means that it has reached its carrying capacity. In nature a levelling occurs too (e.g. Reynolds *et al.*, 2000), for example if nutrient limitation occurs i.e. when there are not enough nutrients available for further increase in phytoplankton density (e.g. Mei *et al.*, 2009; Seppälä *et al.*, 1999). Although not considered in this model, self shading in phytoplankton, which occurs when a large amount of phytoplankton is present in the water column, preventing other phytoplankton from getting enough light to continue growing, can also cause a levelling in phytoplankton density (e.g. Mei *et al.*, 2009; Huisman and Weissing, 1995). The phytoplankton density in the model stays at the level of carrying capacity because apart from the natural mortality there is no other factor defined to reduce its density.

4.2. The NPZ model

The analysis of the NPZ model has shown the presence of a limit cycle which is causing the cyclic behaviour in the densities of the nutrient, phytoplankton and zooplankton state variables in the system. This cycle can be observed in the graphical representation of the numerical integration of the model. The cycle corresponds to the following biological sequence. An increase in the phytoplankton density results in a decrease of the nutrient concentration because the phytoplankton is taking up the nutrients when it is growing. As the phytoplankton density increases the zooplankton density is starting to increase because its food source is increasing. As zooplankton densities are increasing further it starts to control the phytoplankton density. Eventually the zooplankton density becomes so high that it causes the phytoplankton density to decrease further. Once there is not enough phytoplankton left to support the zooplankton it starts to decrease in density. In the process it starts to release the nutrients which means the nutrient concentration is

increasing which enables the phytoplankton density to increase again. This restarts the cycle. This cyclic behaviour has been observed in other models. Examples for this are the models by Steele and Henderson (1992) and Edwards and Brindley (1996) which observed cyclic behaviours in NPZ models over a wide range of parameter values and a range of formulations used.

Cycles have not only been observed in outputs of models they have also been observed in the natural world. In freshwater habitats a cycling between zooplankton and phytoplankton has been observed in analysed data from 30 studies in 12 countries and internally forced oscillations have been found in 15 cases (McCauley and Murdoch, 1987). Cycles have also been observed by Scheffer *et al.* (1997) who looked at the phytoplankton dynamics of Dutch lakes and suggested that the dips in phytoplankton density are caused by zooplankton. They also summarised other studies which showed this phytoplankton - zooplankton interaction. More recently a seasonal phytoplankton zooplankton cycle has been observed in the coastal waters of the Canary Islands (Aristegui *et al.*, 2001) and a cyclic behaviour for most zooplankton species has also been observed in the North Sea (Fransz *et al.*, 1991). While most studies on cycling in populations has been carried out in fresh water habitats, there is also evidence that cycling does occur in the ocean. The reason why cycles in phytoplankton are not commonly observed could be that the more turbulent environment could act to conceal signals which identify cycles (Edwards and Brindley, 1999; Koszalka *et al.*, 2007). In field studies it is difficult to be certain, if the cycles found to occur are due to internal or external forcing. The model used in this study shows that internal forcing can cause cycles.

At the internal equilibrium around which the cycle moves the zooplankton density is higher than the phytoplankton density. This can be explained by the top-down control exerted on the phytoplankton by the zooplankton (Frank *et al.*, 2007). Although the model is minimalist, it is able to replicate the oscillations which have been observed in both laboratory and field experiments (Scheffer *et al.*, 2000).

4.3. The NPZF model

When the fish state variable was added to the previous system, with one internal unstable equilibrium and a stable limit cycle changed to a system with two internal equilibria, of which one was observed to be stable. This finding of an increase in stability with complexity is in agreement with other studies. Scheffer (1991) found that the presence of planktivorous fish has a stabilising effect on the system, with fish dampening the phytoplankton-zooplankton oscillations. It is also in agreement with the work carried out by Smetacek and Nicol (2005) who also found that a predatory population can exert a stabilising effect on populations of shorter lived organisms of lower trophic levels. This finding is also in agreement with more general studies such as the one carried out by Christensen *et al.* (2000) which suggest that the presence of an additional trophic level increases the possible food chain length, which results in a more stable ecosystem.

The analysis of the NPZF system showed a bistability with a basin boundary present. Above the boundary value all the state variables in the system move towards the stable equilibrium in the system in which nutrients, phytoplankton, zooplankton and fish coexist.

The most interesting difference between the stable equilibrium and the unstable equilibrium is that the stable equilibrium point has a higher density of fish. This could be compared to the situation in the natural world where an ecosystem with more fish is stable and becomes unstable as fish are lost from the system for example through fishing. This finding is in agreement with other studies which showed that fishing can have an influence on ecosystem stability (e.g. Jackson *et al.*, 2001).

The stable equilibrium also has a higher phytoplankton density and a lower nutrient concentration than occurs at the unstable equilibrium. This finding in the presence of a lower fish density is a sign of top-down control being exerted by the fish, on the rest of the food chain. This is in agreement with the results obtained in lake experiments which were carried out by Moss *et al.* (2004) which found that if zooplankton are released from

predation pressure they can control the phytoplankton populations, resulting in lower phytoplankton densities in lakes with lower fish biomass than in lakes with higher fish biomass. In lakes with higher fish biomass zooplankton was controlled and phytoplankton was released from grazing pressure resulting in the higher phytoplankton biomass. This finding is also in agreement with the theoretical study carried out by Scheffer et al (2000), which used a classical minimal Daphnia-algae model. This finding also shows that over-fishing will have consequences throughout the pelagic food web (e.g. Frank *et al.*, 2005; Myers *et al.*, 2007). Such a non-linear effect of fish has also been mentioned in other studies (e.g. Megrey *et al.*, 2007).

Below a certain value of fish the behaviour stays in the boundary basin and is not able to reach the stable equilibrium. The fish density goes to zero and then cycles in the nutrient, phytoplankton and zooplankton densities. A reason for a decrease in fish density in the system for example is exploitation through fishing. Empirical data studies have suggested that over-fishing can shift an ecosystem from one state to the other (Daskalov, 2007). Even though a lot of work has been carried out on regime shifts the complexity of ecosystems makes it difficult to find a definitive answer as to what factors are triggering the shifts. However, fishing appears to be a factor in the event of regime shifts (Daskalov, 2007), but so far evidence that the shift is caused by over-fishing has only been circumstantial (Collie *et al.*, 2004).

The finding of a basin boundary in the system of this study is interesting in itself. The observation that the fish density has to be above a critical value to be able to reach the stable equilibrium point could explain an observation in the natural world in which fishery stocks have not recovered from over-exploitation even after closing fisheries stopped exploitation. An example for such a situation is the Newfoundland cod fishery. In 1960s the Canadian cod stock numbered almost two billion individuals but over the last three generations the stock declined by 97%. By 1992 the stock had become commercially extinct and the fishery was closed, but stocks have not recovered despite the closure of the fishery (Hutchings and Reynolds, 2004).

5. Conclusion

The main conclusion that can be taken from this study is that simple models like those analyzed here can be used to gain a better understanding about the processes going on in the interactions between nutrients, phytoplankton, zooplankton and fish groups. The model enables the suggestion of alternative explanations to observations, which have been made in the natural world. It can also provide us with an insight to understanding mechanisms, which are more difficult to understand (Scheffer, 1999), such as factors triggering regime shifts in marine ecosystems. This study gives support to previous studies suggesting that fishing alters ecosystems, and can shift ecosystems from one state to another. Fishing impacts cascade through the food web and that some systems cannot recover after over-exploitation. The findings of this study also give support to the end-to-end modelling approach of ecosystem modelling because they enable to study the impacts of fishing on the whole ecosystem and showed that fish dynamics are influencing plankton dynamics and vice versa.

Future work in this area of work should focus on investigating, which changes occur in the behaviour of system dynamics when the fish state variable is modeled with inclusion of a complete life cycle. This is important because fish have different rates of mortality at different stages of their life cycle and their exploitation is life cycle stage dependent too. The inclusion of the whole life cycle could provide more understanding on which processes are influencing the dynamics in the system and how they influence it.

Acknowledgements

This work was funded through the seedcorn project fund by Cefas. I express my sincere gratitude to my supervisors Richard Law, Jon Pitchford and Steve Mackinson for their support throughout my work.

I also want to thank all the people I have met during my time at York especially the people in D008.

Last but not least I want to thank my family for all their love, support and encouragement.

References

Anonymous (2005) Report of the study group on multispecies assessment in the Baltic (SGMAB). Report ICESCM 2005/H:06, ICES

Andersen K.P. and Ursin E. (1977) A multispecies extension to the Beverton and Holt theory of fishing with accounts of phosphorus circulation and primary production, *Meddr. Danm. Fisk.-og Havunders.*, 7, 319–435

Aristegui J., Hernandez-Leon S., Montero M.F. and Gomez M. (2001) The seasonal planktonic cycle in coastal waters of the Canary Islands, *Scientia Marina*, 65 (Suppl. 1), 51-58

Benndorf J. and Recknagel F. (1982) Problems of application of the ecological model salmo to lakes and reservoirs having various trophic states, *Ecological Modelling*, 17, 129-145

Breck J.E. (1993) Foraging Theory and Piscivorous Fish: Are Forage Fish Just Big Zooplankton?, *Transactions of the American Fisheries Society*, 122, 902-911

Christensen V., Walters C.J. and Pauly D. (2000) Ecopath with Ecosim - A User's Guide. University of British Columbia, Fisheries Centre, Vancouver, Canada and ICLARM, Penang, Malaysia, 131 pp.

Cury P.M., Shin Y.-J., Planque B., Durant J.M., Fromentin J.-M., Kramer-Schadt S., Stenseth N.C., Travers M. and Grimm V. (2008) Ecosystem oceanography for global change in fisheries, *Trends in Ecology and Evolution*, 23, 338-346

Collie J.S., Richardson K. and Steele J.H. (2004) Regime shifts: Can ecological theory illuminate the mechanisms?, *Progress in Oceanography*, 60, 281-302

Daskalov G.M., Grishin A.N., Rodionov S. and Mihneva V. (2007) Trophic cascades triggered by overfishing reveal possible mechanisms of ecosystem regime shifts, *Proceedings of the National Academy of Sciences*, 104, 10518-10523

deYoung B., Heath M., Werner F., Chei F., Megrey B. and Monfray P. (2004) Challenges in modelling ocean basin ecosystem, *Science*, 304, 1463-1466

Díaz López B., Bunke M. and Shirai J.A. (2008) Marine aquaculture off Sardinia Island (Italy): ecosystem effects evaluated through a trophic mass-balance model, *Ecological Modelling*, 212, 292-303

Edelstein-Keshet L. (1988) *Mathematical Models in Biology*, Random House, New York

Edwards A.M. and Brindley J. (1996) Oscillatory behaviour in a three-component plankton population model, *Dynamics and Stability of Systems*, 11, 347-370

Edwards A.M. and Brindley J. (1999) Zooplankton Mortality and the Dynamical Behaviour of Plankton Population Models, *Bulletin of Mathematical Biology*, 61, 303–339

Fennel W. (2008) Towards bridging biogeochemical and fish-production models, *Journal of Marine Systems*, 71, 171-194

Fennel W. (2009) Parameterizations of truncated food web models from the perspective of an end-to-end model approach, *Journal of Marine Systems*, 76, 171-185

Fennel W. and Osborn T. (2005) A unifying framework for marine ecological model comparison, *Deep-Sea Research II*, 52, 1344–1357

Folke C., Carpenter S., Walker B., Scheffer M., Elmqvist T., Gunderson L. and Holling C. (2004) Regime shifts, resilience, and biodiversity in ecosystem management, *Annual Review of Ecology, Evolution, and Systematics*, 35, 557-581

Frank K.T., Petrie B., Choi J.S. and Leggett W.C. (2005) Trophic cascades in a formerly cod-dominated ecosystem, *Science*, 308,1621–1623

Frank K.T., Petrie B. and Shackell N.L. (2007) The ups and downs of trophic control in continental shelf ecosystems, *Trends Ecology and Evolution*, 22, 236–242

Franks P.J.S. (2002.) NPZ models of plankton dynamics: their construction, coupling to physics and application. *Journal of Oceanography*, 58, 379–387

Fransz H.G., Colebrook J.M., Gamble J.C. and Krause M. (1991) the zooplankton of the north sea, *Netherlands Journal of Sea Research*, 28, 1-52

Gehring T.M. and Swihart R.K (2003) Body size, niche breadth, and ecologically scaled responses to habitat fragmentation: mammalian predators in an agricultural landscape, *Biological Conservation*, 109, 283-295

Grimm V. and Railsback S.F. (2005) Individual-based Modelling and Ecology, Princeton University Press

Harley C.D.G., Hughes A.R., Hultgren K.M., Miner B.G., Sorte C.J.B., Thornber C.S., Rodriguez L.F., Tomanek L. and Williams S.L. (2006) The impacts of climate change in coastal marine systems, *Ecology Letters*, 9, 228-241

Hermann A., Hinckley S., Megrey B. and Napp J. (2001) Applied and theoretical considerations for constructing spatially explicit individual-based models of marine larval fish that include multiple trophic levels, *ICES Journal of Marine Science*, 58, 1030-1041

Hjort J. (1914) Fluctuations in the great fisheries of northern Europe viewed in the light of biological research. Rapp. P.-V. Réun, *ICES Journal of Marine Science*, 20, 228

Huisman J. and Weissing F.J. (1995) competition for nutrients and light among phytoplankton species mixed in the water column: theoretical studies, *Water Science and Technology*, 32, 143-147

Hutchings J.A. and Reynolds J.D. (2004) Marine Fish Population Collapses: Consequences for Recovery and Extinction Risk, *BioScience*, 54, 297–309

IMBER (2005) Science Plan and Implementation Strategy. IGBP Report No. 52, IGBP Secretariat, Stockholm. 76 p.

Ito S., Kishi M., Kurita Y., Oozeki Y., Yamanaka Y., Megrey B. and Werner F. (2004) Initial design for a fish bioenergetics model of Pacific saury coupled to a lower trophic ecosystem model, *Fisheries Oceanography*, 13, 111–124

Jackson J.B.C., Kirby M.X., Berger W.H., Bjorndal K.A., Botsford L.W., Bourque B.J., Bradbury R.H., Cooke R., Erlandson J. and Estes J.A. (2001) Historical over fishing and the recent collapse of coastal ecosystems, *Science*, 293, 629–638

Jongejans E., Skarpaas O. and Shea K. (2008) Dispersal, demography and spatial population models for conservation and control management, *Perspectives in Plant Ecology, Evolution and Systematics*, 9, 153-170

Koszalka I., Bracco A., Pasquero C., and Provenzale A. (2007) Plankton cycles disguised by turbulent advection, *Theoretical Population Biology*, 72, 1-6

Koné V., Machu E., Penven P., Andersen V., Garçon V., Demarcq H. And Freon P. (2005) Modelling the primary and secondary productions of the Southern Benguela

upwelling system: a comparative study through two biogeochemical models, *Global Biogeochemical Cycles*, 19, GB4021

Latour R., Brush M. and Bonzek C. (2003) Toward ecosystem-based fisheries management : Strategies for multispecies modelling and associated data requirements, *Fisheries*, 28, 10-22

McCauley E. and Murdoch W.W. (1987) Cyclic and stable populations: plankton as paradigm, *American Naturalist*, 129, 97–121

Megrey B.A. and Kishi M.J. (2002) Model/REX Workshop to Develop a Marine Ecosystem Model of the North Pacific Ocean Including Pelagic Fishes, *PICES Scientific Report*, 20, 77–176

Megrey B., Rose K., Klumb R., Hay D., Werner F., Eslinger D. and Smith L. (2007) A bioenergetic/population dynamics model of Pacific herring (*Clupea harengus pallasii*) coupled to a lower trophic level nutrient-phytoplankton-zooplankton model: Dynamics, description, validation and sensitivity analysis, *Ecological Modelling*, 202, 144-164

Mei P., Finkel Z.V., Irwin A.J. (2009) Light and nutrient availability affect the size scaling of growth in phytoplankton, *Journal of Theoretical Biology*, 259, 582–588

Moss B., Stephen D., Balayla D., Bécares E., Collings S.E., Fernandez-Aláez C., Fernández-Aláez M., Ferriol C., Garcia P. and Gomá J. (2004) Continental-scale patterns of nutrient and fish effects on shallow lakes: synthesis of a pan-European mesocosm experiment, *Freshwater Biology*, 49, 1633-1649

Murray A.G. and Parslow J.S. (1999) The analysis of alternative formulations in a simple model of a coastal ecosystem, *Ecological Modelling*, 119, 149–166

Myers R.A., Baum J.K., Shepherd T.D., Powers S.P. and Peterson C.H. (2007) Cascading effects of the loss of apex predatory sharks from a coastal ocean, *Science*, 315, 1846–1850

Otto S.P. and Day T. (2007) A biologist's guide to mathematical modelling in ecology and Evolution, Princeton university Press, Oxford

Pope J.G. (1979) A Modified Cohort Analysis in Which Constant Natural Mortality is Replaced by Estimates of Predation Levels. ICES C.M. 1979/H, 16p.

Rantalainen M.-L., Haimi J., Fritze H., Pennanen T. and Setälä H. (2008) Soil decomposer community as a model system in studying the effects of habitat fragmentation and habitat corridors, *Soil Biology and Biochemistry*, 40, 853-863

Reynolds C.S., Reynolds S.N., Munawar I.F. and Munawar M. (2000) The regulation of phytoplankton population dynamics in the world's largest lakes, *Aquatic Ecosystem Health and Management*, 3, 1-21

Scheffer M. (1991) Fish and nutrients interplay determines algal biomass: a minimal model, *Oikos*, 62, 271-282

Scheffer M. (1999) Searching explanations of nature in the mirror of math, *Conservation Ecology*, 3, article 11

Scheffer M., Rinaldi S., Kuznetsov Y.A. and van Nes E.H. (1997) Seasonal dynamics of Daphnia and algae explained as a periodically forced predator-prey system., *Oikos*, 80, 519-532

Scheffer M., Rinaldi S. and Kuznetsov YA.. (2000) The effect of fish on plankton dynamics: a theoretical analysis, *Canadian Journal of Fisheries and Aquatic Sciences*, 119, 149-166

Seppälä J., Tamminen T. and Kaitala S. (1999) Experimental evaluation of nutrient limitation of phytoplankton communities in the Gulf of Riga, *Journal of Marine Systems*, 23, 107–126

Shea K. and the NCEAS Working Group on Population Management (1998) Management of populations in conservation, harvesting and control, *Trends in Ecology & Evolution*, 13, 371-375

Smetacek V. and Nicol S. (2005) Polar ocean ecosystems in a changing world, *Nature*, 437, 362-368

Soetaert K. and Herman P.M.J. (2009) A Practical Guide to Ecological Modelling using R as a Simulation Platform, Springer

Steele J.H. and Henderson E.W. (1992) The role of predation in plankton models, *Journal of Plankton Research*, 14, 157-172

Stigebrandt A., Aure J., Ervik A. and Hansen P.K. (2004) Regulating the local environmental impact of intensive marine fish farming. III. A model for estimation of the holding capacity in the Modelling-Ongrowing Fish Farm-Monitoring System, *Aquaculture*, 234, 289–261

Travers M. (2009) PhD Thesis Couplage de modules trophiques et effets combinés de la pêche et du climat, Docteur de L'Université Pierre et Marie Curie

Travers M., Shin Y.-J., Jennings S. and Cury P. (2007) Towards end-to-end models for investigating the effects of climate and fishing in marine ecosystems, *Progress in Oceanography*, 75, 751- 770

Travers M., Shin Y.-J., Jennings S., Machu E., Huggett J.A., Field J.G. and Cury P.M. (2009) Two-way coupling versus one-way forcing of plankton and fish models to predict ecosystem changes in the Benguela, *Ecological Modelling*, 220, 3089-3099

Truscott J.E. and Brindley J. (1994) Equilibria, Stability and Excitability in a General Class of Plankton Population Models, *Philosophical Transactions: Physical Sciences and Engineering*, 347, 703-718

Vieira J.M.P. and Lijklema L. (1989) Development and application of a model for regional water quality management, *Water Research*, 23, 767-777

Werner F.E., Ito S-I, Megrey B.A. and Kishid M.J. (2007) Synthesis of the NEMURO model studies and future directions of marine ecosystem modelling, *Ecological Modelling*, 202, 211–223